Journal of Power Sources 185 (2008) 248–260

Contents lists available at ScienceDirect

Journal of Power Sources

journal homepage: www.elsevier.com/locate/jpowsour

Experimental analysis of internal gas flow configurations for a polymer electrolyte membrane fuel cell stack

A. Friedl*, S.D. Fraser, W.R. Baumgartner, V. Hacker

Graz University of Technology, Institute for Chemistry and Technology of Inorganic Materials, CD-Laboratory for Fuel Cell Systems, Steyrergasse 21, 8010 Graz, Austria

ARTICLE INFO

Article history:
Received 22 April 2008
Received in revised form 4 June 2008
Accepted 6 July 2008
Available online 15 July 2008

Keywords:
Fuel cell stack
Gas flow configuration
Stack design
Polymer electrolyte membrane
PEMFC

ABSTRACT

The internal gas distribution system utilised for supplying fresh reactants and removing reaction products from the individual cells of a fuel cell stack can be designed in a parallel, a serial or a mixture of parallel and serial gas flow configuration. In order to investigate the interdependence between the internal stack gas distribution configuration and single cell as well as overall stack performance, a small laboratory-scale fuel cell stack consisting of identical unit cells was subject to operation with different gas distribution configurations and different operating parameters. The current/voltage characteristics measured with the different gas distribution configurations are analysed and compared on unit cell- as well as on stack-level. The results show the significant impact of the internal stack gas distribution system on operation and performance of the individual unit cells and the overall stack.

1. Introduction

Fuel cells are a promising option for replacing state-of-the-art energy conversion and storage technologies such as internal combustion engines and batteries due to their high conversion efficiency and their low- or even zero-emission operation. Today's fuel cell technology is still too expensive and does not yet provide the durability required to replace established power generation and energy storage technologies in most applications, though [1]. One of the key issues in developing cost-competitive and durable fuel cell systems is the fuel cell stack design.

Generally, a fuel cell stack is built from a number of individual cells. These individual cells are normally electrically connected in series to provide a useful stack output voltage. The internal gas distribution system required to supply fresh reactants to the cells and to subsequently remove reaction products from the cells can essentially be designed in a parallel, a serial or a mixture of parallel and serial gas flow configuration. Individual cells operated in a parallel gas flow configuration ideally receive identical input gas streams whereas the outlet gas stream of one cell is the inlet gas stream of the downstream cell in a serial gas flow configuration.

Most fuel cell stacks in the medium and high output power range are either based on a fully or at least partially parallel gas flow configuration, where the fuel cell stack inlet gas stream is divided into more or less identical gas streams that are fed to the individual cells. Two typical parallel gas distribution systems, the U- and the Z-manifolds are discussed in Park and Li [2], Chang et al. [3] and in Koh et al. [4] (in a U-manifold, gas outlet and gas inlet are on the same side of the stack; in a Z-manifold, gas outlet and gas inlet are on opposite sides of the stack). A parallel gas flow configuration has the advantage of – at least in theory – supplying identical input gas streams to each of the cells. This simplifies input gas conditioning because the fuel and air input gas streams can be equally optimised for all of the cells, e.g. with respect to temperature and humidity at the same time. In addition, only a small pressure difference between stack inlet and stack outlet is required because each cell only receives the gas flow directly required by the cell (plus an additional small surplus for providing cell operation with stoichiometry rates greater than one), and no surplus gas for downstream cells has to be pumped through the flow fields.

Due to the fact that the gas stream is fed into a number of cells installed in parallel, however, problems may arise due to maldistribution of species within the stack. Owejan et al. [5], for instance, remark that the presence of water slugs in the flow field gas channels can reduce the stoichiometry ratio to values smaller than one, and thus cause a severe cell voltage loss. These maldistribution problems can be reduced if the manifold of a parallel gas distribution approach is optimised to homogenise the gas distribution within the stack [6].

Abbreviations: MEA, membrane electrode assembly; OCV, open circuit voltage; PEMFC, polymer electrolyte membrane fuel cell; r.h., relative humidity.

* Corresponding author. Tel.: +43 3168738785; fax: +43 3168738782.
E-mail address: adina.friedl@tugraz.at (A. Friedl).

0378-7753/$ – see front matter © 2008 Elsevier B.V. All rights reserved.
doi:10.1016/j.jpowsour.2008.07.005

Alternatively, certain aspects associated with the maldistribution of reactants in a parallel gas flow configuration can be reduced or even completely eliminated if a serial gas flow configuration is applied where the gas flow of multiple cells is forced through each of the unit cells installed in the serial configuration. A serial gas flow configuration is, for instance, inevitably linked to higher gas flow rates and pressure differentials because the reactants required by the whole line of serially connected cells has to be transported through the upstream cells. This makes a complete blocking of one of the cells (e.g. due to water slugs) less probable than with a parallel gas flow configuration.

The stream of fresh reactants is gradually consumed and replaced with reaction products as the gas streams flow from the inlet to the outlet cell of a serial gas flow configuration. This makes gas conditioning a major challenge, as each unit cell of a serial configuration receives a different ratio of reactants and reaction products.

A serial gas flow configuration is a particularly interesting option with small fuel cell systems, e.g. designed for portable applications in consumer electronics. Planar fuel cell stacks can thus be designed on a single layer by sequentially feeding the fuel and/or the air gas streams through the individual cells [7,8]. The utilisation of a serial gas flow configuration or the combination of a serial fuel gas and a parallel air gas configuration suggests itself for many of such applications. Such a configuration would combine the high utilisation rates of the serial fuel distribution approach with the high stoichiometry rates provided the low pressure-gradient parallel air flow approach.

The gas flow configuration is an important aspect in the design of a fuel cell stack, as the supply of educts as well as the removal of reaction products have a significant impact on cell and stack operation and performance. The gas flow configuration therefore has to be carefully chosen and optimised with respect to the requirements of a specific application in order to provide an efficient and uniform operation of each individual cell of a fuel cell stack.

The interdependence between cell and stack operation and the internal gas distribution approach is investigated within this paper. This analysis is based on an experimental study made with a small laboratory-scale fuel cell stack consisting of identical unit cells. The unit cells were operated in a total of six different gas distribution configurations. The results derived from these investigations provide a valuable insight into possibilities and limitations of different gas distribution configurations.

2. Analysis

2.1. Fuel cell performance degradation effects

The shelf life of a fuel cell system operated in a real-world application essentially depends on two major aspects: durability and stability [9]. A high durability enables fuel cell operation over long periods without complete system failures. The stability of a fuel cell, however, is reflected by the performance degradation occurring during as well as in-between the operational periods. Due to the fact that the operational output voltage of a fuel cell is proportional to the efficiency of the fuel-to-electric conversion process, the performance of a fuel cell is normally represented by the output voltage available at the electrical terminals of a single cell or stack. A low stability will therefore normally result in a reduction of the operational fuel cell output voltage.

Basically, one can distinguish between a recoverable and unrecoverable degradation effect. Recoverable degradation effects are caused by temporary and reversible changes in performance (e.g. electrode flooding; membrane drying; changes in the catalyst surface oxidation state). Degradation effects are unrecoverable if corrective measures are not taken in time and the cell is therefore irreversibly damaged (e.g. dissolution, migration or sintering of the catalyst; oxidation of the carbon support material; loss of catalyst–ionomer–reactant three-phase regions; membrane weakening; delamination of MEA layers; holes in the membrane; corrosion of the bipolar plates) [9–11]. A poor stability will inevitably lead to a low durability and therefore limit the use of the fuel cell system in real-world applications.

Three effects causing performance degradation of polymer electrolyte membrane fuel cells (PEMFCs) are specifically investigated within this work: electrode flooding, drying of the membrane and depletion of reactants in the fuel and air gas streams. Each of these effects leads to an immediate but fully reversible loss in cell output voltage as long as the cell is not subject to operation under extreme local operating conditions. Blocking of gas channels may lead to irreversible cell degradation due to the presence of extremely high local current densities in the remaining operational active cell area. Baumgartner et al. [10], for instance, investigated the effect of fuel cell operation at hydrogen starvation conditions with a laboratory cell that is based on the same design that has also been applied with the unit cells applied within this work. Hydrogen starvation would, e.g. occur if parts of a cell or even a whole cell cannot be supplied with sufficient quantities of fresh hydrogen because, e.g. water slugs block gas channels.

Baumgartner et al. measured significant carbon dioxide emissions due to the presence of strong degradation effects under hydrogen starvation operation when the whole current output of a cell is generated in just a fraction of the total active cell area.

Effects causing irreversible cell performance degradation (e.g. corrosion of the carbon catalyst support) or degradation phenomena only present with long-term operation of the cell (e.g. migration or sintering of the catalyst particles) are not considered in this work.

The interdependencies between the three aforementioned performance degradation effects are shown in Fig. 1. Within this work, the fuel cell performance is considered to be directly proportional to the operational cell or stack output voltage available for certain operating conditions. As mentioned above, this is due to the fact that the efficiency of a fuel cell is proportional to the operational output voltage; a loss in operational output voltage will increase the fuel consumption required to provide a certain electrical output power. Losses associated with balance of plant components such as compressors or blowers are not considered within this work.

Depletion of reactants in the fuel and air gas streams leads to a reduction in fuel cell output voltage because the Nernst potential is reduced [12], and mass transport limitations result in additional concentration overvoltages that further reduce the operational output voltage of the cell or stack [13–16]. Electrode flooding and drying of the membrane are directly related to the water balance between membrane, electrodes and the (externally humidified) fuel and air gas streams [17,18]. If too much water (vapour) is present within the cell or stack, water vapour can condensate and partially or even fully block the porous gas diffusion electrodes and the gas channels. This will hamper or even fully prevent the supply of fresh reactants to the electrochemically active sites [19].

The opposite effect can occur if a low-temperature PEMFC does not hold sufficient quantities of water. In this case, the membrane can dry out and the ohmic drop across the membrane will increase significantly [20–22]. Membrane drying can even lead to irreversible degradation effects, e.g. if certain regions of a cell or certain cells of a stack (e.g. the cells located in the middle of a stack) are overheated because the heat produced by ohmic heating cannot be removed efficiently [23].

Countermeasures exist to reduce the losses associated with each of the three aforementioned effects. A loss in fuel cell output voltage

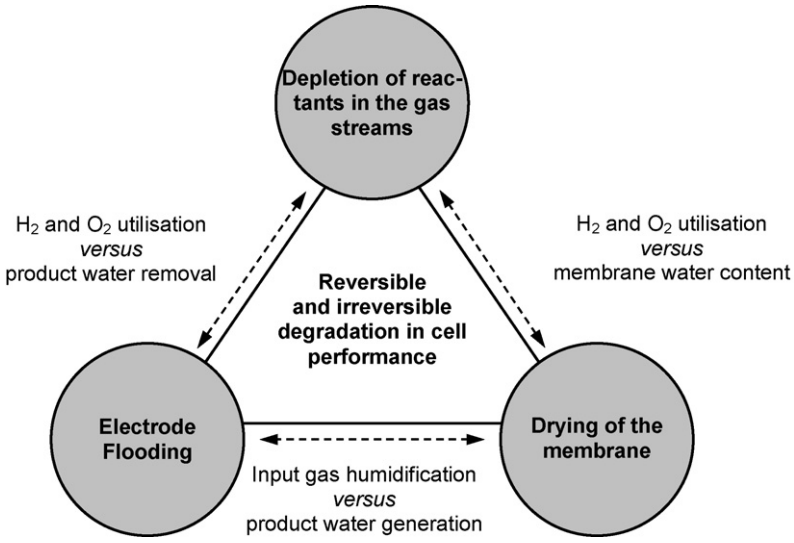

Fig. 1. Investigated performance degradation phenomena causing an immediate and reversible loss in cell or stack output voltage.

due to depletion of active reactants in the fuel and air gas streams can often be significantly reduced or even eliminated by increasing the stoichiometry of the fuel and air gas streams. Thus, more active reactants are supplied to the cell and the average concentration of fuel and oxygen in the active cell regions can be increased. Electrode flooding can be avoided by increasing the gas flow rates and/or by reducing the relative humidity (r.h.) of the input gas streams. Thus, more product water can be removed out of the cell by the output gas streams. The opposite has to be done to avoid drying of the polymer electrolyte membrane. In this case, the input gas flow rate can be reduced and/or the relative humidity of the input gas streams can be increased. Thus, the net removal of water out of the fuel cell can be reduced and sufficient quantities of water can remain within the cell to keep the polymer electrolyte membrane well-humidified.

2.2. Operating parameters

Basically, there are four different variables in fuel cell operation that can be modified to maximise the fuel cell output voltage for a given cell output current: fuel and air stoichiometry as well as the relative humidity of the fuel and air input gas streams. Within this study, we assume that the temperature of the fuel and air input gas streams is equal to the controlled and constant temperature of the fuel cell stack; if this was not the case, the temperatures of the input gas streams as well as the fuel cell stack could also be modified. This was not considered within this study, though.

Moving up from individual cell- to stack-level, an additional variable determining the operational stack output voltage is available: the internal gas flow configuration of the stack. Basically, three different approaches in fuel cell stack gas flow configuration are possible: a parallel gas flow configuration where each cell is supplied with identical input gas streams; a serial gas flow configuration where the output gas stream of one cell is utilised as input gas stream of the downstream cell; and finally a mixed gas flow configuration where some of the cells are installed in a parallel, and some of the cells are installed in a serial gas flow configuration. Assuming that the flow field patterns of the anode and cathode electrode are identical, each configuration can be operated in a co-flow mode (fuel and air gas streams flow into the same direction) or in a counter-flow mode (fuel and air gas streams flow into the opposite directions). If the flow field patterns of the anode and cathode are not identical, a distinction between co- and counter-flow mode is possible by comparing the general flow direction of the fuel and air gas streams. The laboratory-scale single cells utilised within this study have identical flow field patterns on the anode and cathode electrode. The cells can thus be operated in co- and counter-flow mode.

The internal gas flow configuration has a significant impact on the operational characteristics of the individual cells and the overall fuel cell stack, respectively. Considering that in an all-serial configuration all of the active reactants of the downstream cells as well as the product water of all upstream cells has to be transported through a single cell, this will obviously result in a completely different fuel and air stoichiometry as well as water balance than in an all-parallel configuration, where each cell is supplied with identical gas streams.

The focus of this work is to investigate the variation in fuel cell stack performance as a function of the internal gas flow configuration for different values of stoichiometry and relative humidity of the fuel and air input gas streams. Thus, the interdependencies between cell and stack performance and a total of six investigated gas flow configurations can be investigated. These interdependencies are the key in determining possibilities and limitations of the different fuel cell stack internal gas flow configurations, as presented in Fig. 2.

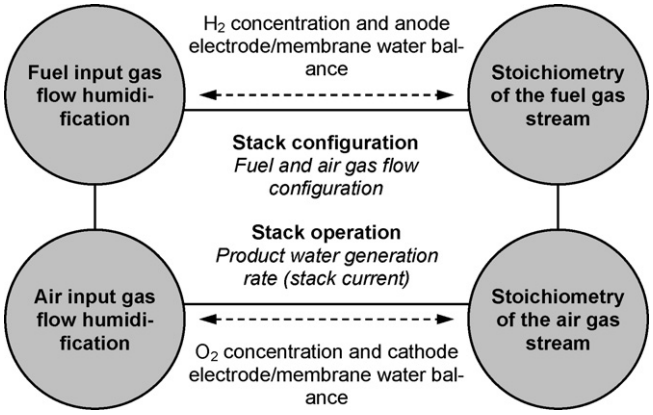

Fig. 2. Fuel cell operating parameters investigated within this study.

(a)

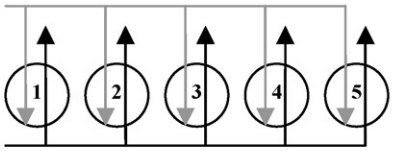

Stack setup 1: all-parallel gas flow configuration of five cells, counter-flow mode.

(b)

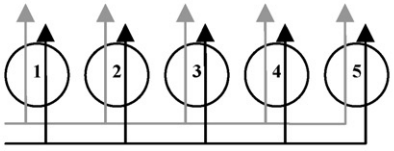

Stack setup 2: all-parallel gas flow configuration of five cells, co-flow mode.

(c)

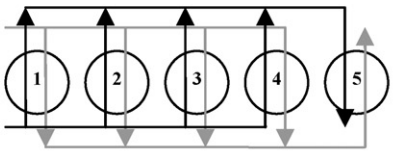

Stack setup 3: serial gas flow configuration of four parallel and one single cell in counter-flow mode.

(d)

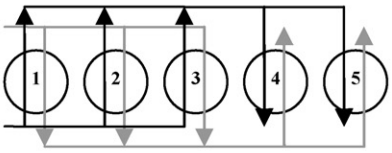

Stack setup 4: serial gas flow configuration of three and two parallel cells in counter-flow mode.

(e)

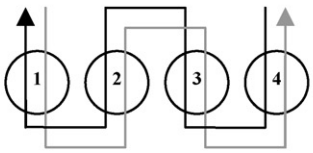

Stack setup 5: all-serial gas flow configuration of four cells, counter-flow mode.

(f)

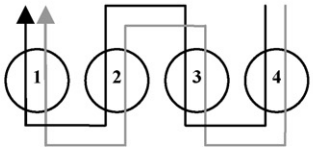

Stack setup 6: all-serial gas flow configuration of four cells, co-flow mode.

Fig. 3. Schematic view of the six different internal stack gas flow configurations (black arrows corresponds to the anode flow direction; grey arrows correspond to the air flow direction). Stack setup 1: all-parallel gas flow configuration of five cells, counter-flow mode. (b) Stack setup 2: all-parallel gas flow configuration of five cells, co-flow mode. (c) Stack setup 3: serial gas flow configuration of four parallel and one single cell in counter-flow mode. (d) Stack setup 4: serial gas flow configuration of three and two parallel cells in counter-flow mode. (e) Stack setup 5: all-serial gas flow configuration of four cells, counter-flow mode. (f) Stack setup 6: all-serial gas flow configuration of four cells, co-flow mode.

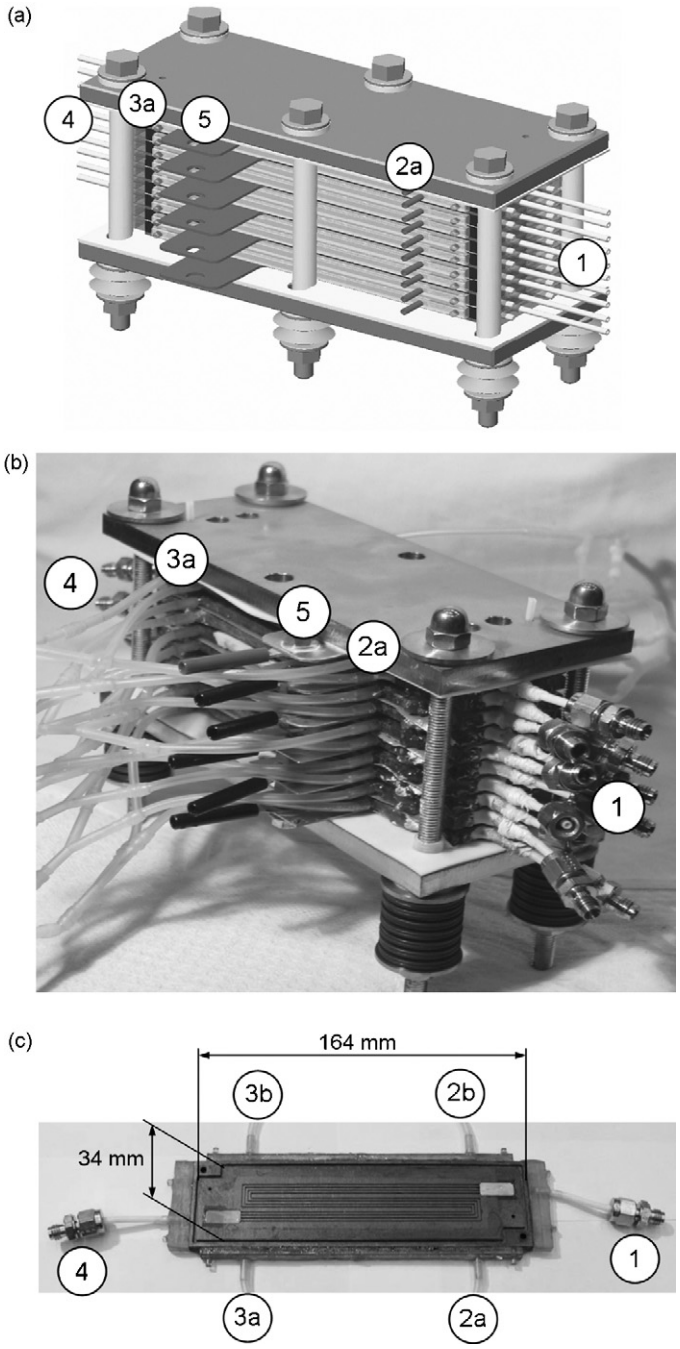

Fig. 4. (a) Schematic view of the fuel cell stack; (b) picture of the fuel cell stack prior to installation; (c) picture of the flow field plate.

2.3. Internal fuel cell stack gas flow configurations

Different gas flow configurations were investigated within this work by varying the interconnections of the individual and identical cells within the fuel cell stack. The fuel and air gas streams of the individual cells were interconnected in a serial and/or parallel gas flow configuration. The six fuel cell stack gas flow configurations shown in Fig. 3 were investigated within this work. The different fuel cell stack configurations were only modified with respect to the fuel and air gas flow configurations; the individual cells were always electrically operated in a serial configuration, as mentioned above.

Stack setups 1 and 2 are all-parallel gas flow configurations operated in co- and counter-flow mode. Stack setups 5 and 6 are all-serial gas flow configurations operated in counter- and co-flow mode. Stack setups 3 and 4 are mixed setups, comprising of a parallel section of four (setup 3) and three (setup 4) cells operated in parallel, and one (setup 3) and two (setup 4) cells in serial gas flow configuration. Setups 3 and 4 were included in this investigation because a serial configuration of one or more fuel cell modules – each module comprising of a set of individual cells operated in a parallel configuration – is a feasible option that might be a good trade-off between an all-parallel and an all-serial gas flow configuration.

Setups 1–4 were investigated with stacks comprising of five individual laboratory-scale cells. The fifth cell had to be removed from the stack before measuring setups 5 and 6 due to the presence of a hydrogen leak in the cell manifold. Setups 5 and 6 were therefore only investigated with a stack comprising of four individuals cells. A direct comparison of the operational characteristics measured with stack setups 1–6 is nevertheless possible because the stoichiometry of the fuel and air input gas streams was always determined for the actual consumption, i.e. as a function of cell output current, individual cell area, and the number of individual cells installed in the stack. Absolute input gas flow rates of water, active species and nitrogen in setups 5 and 6 were therefore 20% smaller than in setups 1–4. The fact that a different number of cells has been used in the measurements of stack setups 5 and 6 is therefore not of significant relevance when comparing and analysing general trends in operating conditions and cell performance. The resolution of the results determined with the all-serial setups is, however, slightly reduced because the effects can only be monitored in four instead of five individual unit cells.

Each of the fuel cell stack setups 1–6 was operated at a uniform stack temperature of 70 °C (the cell temperatures were controlled by a water cooling system), and a constant fuel stoichiometry (λ_{fuel}) of 1.5 was applied with all measurements. The stoichiometry rate was always computed with respect to the overall fuel cell stack consumption and not with respect to the consumption of the individual cell(s) the input gas was supplied to; the gas input cell of a serial gas flow configuration was therefore supplied with stoichiometry rates in excess of 1.5, whereas cells operated in all-parallel configurations were supplied with a fuel stoichiometry rate of exactly 1.5, for instance.

The constant fuel stoichiometry of 1.5 was chosen because this value is the standard value applied with all PEMFC measurements made within the authors' laboratory investigations. The fuel stoichiometry is generally rather chosen for a specific fuel cell system or application (e.g. open loop or closed loop anode gas feed) and not for specific operating conditions. Due to the fact that the supply of hydrogen is often limited to the volume stored within a storage vessel, the hydrogen stoichiometry will normally rather be minimised for a specific application, rather than choosing a higher stoichiometry that will inevitably result in a lower utilisation rate if an open loop fuel gas feed is applied. The stoichiometry of the air flow, on the other hand, can be varied over a wide range due to the unlimited supply of ambient air.

The relative humidity of the fuel and air input gas streams as well as the stoichiometry of the air input gas stream were changed within the measurement series to investigate the interdependencies between single cell and overall fuel cell stack performance as a function of the operating conditions. All fuel cell stack configurations were operated with relative humidities of 0/90%, 60/60%, 90/90% (relative humidity of the fuel/air input gas streams). The stoichiometry of the air flow (λ_{air}) was set to values of 1.4, 1.8, 2.2, 2.6 and 3.0.

Table 1
Overview of cell and stack properties

MEA	GORE PRIMEA 5620 Series
Active cell area	25 cm^2
Platinum content, anode	0.4 mg_{Pt} cm^{-2}
Platinum content, cathode	0.6 mg_{Pt} cm^{-2}
Gas diffusion layer	SGL Carbon Group GDL 24BC
Bipolar plate	Machined from SGL Carbon Group PPG 86
Flow field	Quadruple serpentine, two bends
Thermal control	Water cooling system installed in bipolar plates

The different stack setups were subsequently analysed by comparing the current/voltage characteristics of the individual cells and the fuel cell stack.

3. Experimental set-up and procedure

3.1. Experimental set-up

All of the measurements were made with a laboratory-scale PEMFC stack consisting of a number of individual cells (five individual cells were utilised with stack setups 1–4; four individual cells were utilised with stack setups 5 and 6, as discussed above). The single cells were developed and manufactured within the authors' laboratory and have an active cell area of 25 cm^2 each. These laboratory-scale single cells are utilized with a wide range of different investigations within the authors' research facility [24–26]. Each individual cell has a water-based thermal management system to maintain a constant temperature of 70 °C during operation. Commercially available membrane electrode assemblies (MEAs) were applied within this work.

The individual cells were electrically connected in series with all investigated stack setups. Each individual cell has separate input and output lines for the fuel and air gas streams. Thus, a quick and easy switching between different gas flow configurations is possible by simply connecting the different input and output lines of the individual cells in the desired serial and/or parallel gas flow configuration. The stack therefore does not have to be disassembled between measuring different gas flow configurations.

The individual cells are electrically connected in series and installed between two steel end plates. A schematic view of the fuel cell stack is shown in Fig. 4a The fully assembled fuel cell stack is shown in Fig. 4b prior to installation in the test rig. As can be seen in Fig. 4b, the fuel and air input lines, the water cooling system as well as the sockets of the cell voltage measurement were not yet interfaced to the stack. Apart from that, the stack was ready for operation.

A picture of the flow field plate with the quadruple-line serpentine flow field layout is shown in Fig. 4c.

The labels shown in Fig. 4a–c indicate: (1) gas inlet line; (2a, 3a) cooling water inlet lines; (2b, 3b) cooling water outlet lines; (4) gas outlet line; (5) flap on the current collector plate for the cell voltage measurement.

An overview of cell and stack properties is presented in Table 1.

The cells were sealed with two 180-μm thick silicon seals and fixed with six screws and disc springs to provide a reproducible compression force over the whole cell area.

Table 2
Overview of measurement equipment

Electrochemical workstation	Zahner Elektrik IM6ex (for control of PP240)
Potentiostat	Zahner Elektrik PP240
Mass flow controller H_2	M+W Instruments D-5111
Mass flow controller air	Bronkhorst Low-Δp-Flow F-202D
Humidity input gas streams	Computed from water temperature in humidifiers

Table 3
Accuracy of experimental procedure

Accuracy of the potential measurement	±0.1%/±1 mV
Accuracy of the current measurement	±0.25%
Accuracy of the H_2 flow rate	±3% of full scale (incl. linearity)
Reproducibility of the H_2 flow rate	±0.5% of full scale
Accuracy of the air flow rate	±1% of full scale (incl. linearity)
Repeatability of the air flow rate	<0.2% of reading

3.2. Experimental procedure

The anode and cathode flow fields of the individual cells were supplied with humidified hydrogen and humidified air, respectively. Both input gas streams were supplied to the cells at near-ambient pressure. Slight overpressures were only present due to the pressure loss induced by the gas flow within the flow fields and the inter-cell gas connectors (if present). The experimental setup did not enable a direct measurement of the pressure drop required to push the gas streams through the individual cells. An estimate of this pressure drop can be derived on the basis of the input gas flow rates; the input gas flow rates are roughly proportional to the number of cells supplied in series. Strictly speaking, this is only true when comparing parallel cells and the first cell of a serial configuration; downstream cells operated in a serial configuration can receive slightly different gas flow rates as the consumption of the upstream cell(s) has to be considered. Switching from a five-cell all-parallel setup to a five-cell all-serial setup will therefore roughly increase the velocities of the fuel and air gas streams by a factor of five. The Reynolds number will therefore also be correspondingly increased by a factor of five. Based on the (strongly simplified) assumption of an ideal laminar flow regime, the pressure drop will therefore also increase by a factor of five. This is just a very simplified estimate, but nevertheless provides a rough guideline for evaluating the results presented in the following.

Input gas flow rates and humidification levels were controlled with an automated fuel cell test station also developed and manufactured in the authors' laboratory [24,25]. An overview of the measurement equipment applied with the investigation is presented in Table 2. An analysis of the measured properties is presented in Table 3.

An overview of the reference operating parameters utilised with the measurements is presented in Table 4. If operating parameters are not specifically given with the results presented in this paper, the reference operating parameters presented in Table 3 were applied.

This test rig has two heated bubble humidifiers for input gas humidification and is capable of supplying mixtures of hydrogen, nitrogen and oxygen utilising computerized mass flow controllers at a given mass flow rate.

Electrical properties were measured with a Zahner Elektrik impedance measurement station consisting of an IM6ex Electrochemical Workstation and an add-on PP240 Power Potentiostat.

The gas flow rate was controlled and supplied for the whole stack and not for each cell individually. A system-immanent mald-

Table 4
Reference operating parameters

Cell temperature	70 °C
Fuel stoichiometry	1.5
Air stoichiometry	2.2
Fuel pressure	1 bar abs.
Air pressure	1 bar abs.
Anode dry gas molar fraction	H_2: 1.0
Cathode dry gas molar fraction	O_2: 0.21; N_2: 0.79

istribution of the gas flow rates supplied to the individual cells due to differences in cell components and design was avoided as far as possible by carefully machining identical cells with identical gas distribution lines. A time-dependent maldistribution, e.g. due to condensation of water in the offgas lines or due to accumulation within the cells and MEAs, however, cannot be completely avoided with the investigated setup [5].

The measurements were started after an MEA activation procedure at which the cells were operated in six consecutive cycles. Each cycle consisted of a 30-min operation at 10 A, 30 min operation at 20 A and 1 min operation at open circuit voltage (OCV) mode.

Current/voltage characteristics measured with the different stack setups and operating conditions were only considered with the subsequent analyses if stable operation of each cell could be achieved. If stable operating conditions could not be achieved with one or more of the cells, the respective measurements were neither considered in the subsequent analyses nor with the plots presented within this paper.

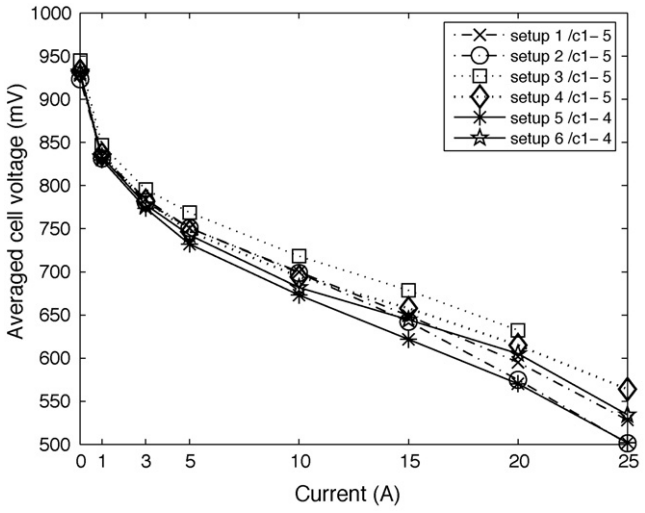

Fig. 5. Comparison of averaged cell output voltages for stack setups 1–6 (70 °C stack temperature, $\lambda_{fuel} = 1.5$, $\lambda_{air} = 2.2$, 90/90% r.h. fuel/air input gas streams).

4. Results and discussion

4.1. Cell and stack performance as a function of internal gas flow configuration

Individual cell and overall stack performance of stack setups 1–6 are analyzed and compared in the following. In order to enable a simple visual distinction between the measured cell characteristics of different stack setups, averaged current/voltage characteristics are computed for all individual cells of a specific stack setup that were operated in parallel gas flow configuration. Individual cells operated in parallel receive identical input gas flow streams, and their current/voltage characteristics are therefore almost identical. Plotting the current/voltage curve of each individual cell of a parallel gas flow configuration separately would therefore only provide redundant information.

Stack setups 1 and 2 are therefore only plotted with one current/voltage curve each, as all five cells were operated in an all-parallel gas flow configuration. Two current/voltage curves are plotted for stack setups 3 and 4, as both of these stack setups feature parallel cells and one (setup 3) or two (setup 4) cells in a serial gas flow configuration. All of the cells operated in stack setups 5 and 6 are plotted individually as there are no cells in parallel gas flow configuration in these two stack setups.

The following notation is applied within the plots: 'setup *X*/c*Y*–*Z*'. X denotes the stack setup (setups 1–6 as shown in Fig. 3). c*Y*–*Z* specifies that the curve gives the averaged cell output voltage of cells *Y*–*Z* of the investigated stack setup *X*. A curve denoted setup 3/c1–4 therefore shows the averaged cell output voltage of cells one to four operated in stack setup 3, for instance.

The current/voltage characteristics presented in Figs. 5 and 6 were made at constant operating conditions (stack temperature of 70 °C, hydrogen stoichiometry of 1.5, air stoichiometry of 2.2 and 90/90% relative humidity of the fuel/air input gas streams).

A comparison of the averaged cell voltages for stack setups 1–6 is presented in Fig. 5.

The measurements revealed that stack setup 3 provides the highest average cell output voltage for all investigated stack output currents. The current/voltage characteristics of stack setups 1, 2 and 4 show very similar characteristics. Stack setup 4, the second stack setup with mixed gas flow configuration besides stack setup 3, provided the highest output voltages of these three stack setups in high current density operation. The lowest average cell output voltages are provided by stack setups 5, one of the two all-serial configurations. Stack setup 6, the second all-serial gas flow configuration provides significantly higher output voltages than stack setup 5.

In order to investigate differences in the current/voltage characteristics of the six different gas flow configurations, the three pairs of related stack setups (i.e. the two all-parallel setups 1 and 2, the two mixed setups 3 and 4 and the two all-serial setups 5 and 6) are individually analysed and compared in the following.

4.1.1. All-parallel gas flow configurations 1 and 2

The measurements only showed a very small difference in current/voltage characteristics between the averaged cell voltages of stack setups 1 and 2, as presented in Fig. 6(a).

The current/voltage curves of stack setups 1 and 2 are almost identical for stack currents up to 10 A. If higher currents are drawn from the stack, co-flow operation (stack setup 2) provides lower average cell output voltages than counter-flow operation (stack setup 1). This slight advantage of the counter- over the co-flow mode is only valid for the investigated operating parameters (stoichiometry rates, input gas stream humidification), though. Measurements made with a different set of operating conditions showed contrary results, as presented with the results of the humidity-dependent investigations, for instance.

The slight advantage of counter- over co-flow operation measured with the investigated set of operating conditions at high output currents could be due to a better water balance of the cells in counter-flow mode. In co-flow operation, the membrane is considerably better humidified in the outlet than in the inlet region due to product water uptake, particularly if the cell is operated with high current densities. This leads to considerable variations in the current density distribution, as the membrane water content is directly related to the conductivity and inversely related to the ohmic drop across the membrane. This effect can often be reduced if the cell is operated in counter-flow mode. The membrane is then again better humidified in the air outlet region due to product water uptake, but the fuel inlet gas stream enters the fuel cell in a cell region where the membrane is already well-humidified and can thus be 'internally humidified' by the membrane. The more homogenous distribution of water over the active cell area (and the resulting more homogenous current density distribution) could explain why counter-flow operation of the cells provides higher cell output voltages than co-flow operation. The differences in average cell output voltages are relatively small between stack setups 1 and 2; the effect of switching from co- to counter-flow mode does therefore

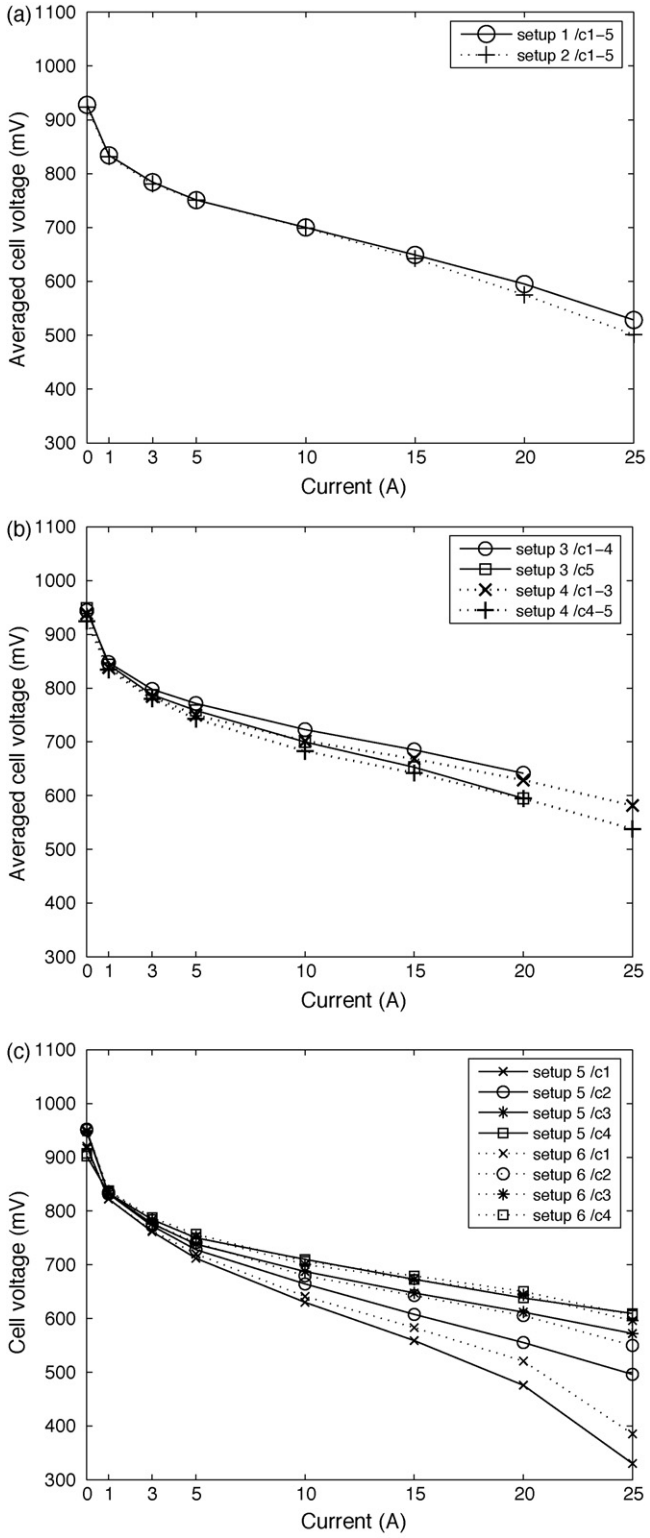

Fig. 6. Comparison of averaged cell output voltages for stack setups 1 and 2 (a); 3 and 4 (b); 5 and 6 (c) (70 °C stack temperature, λ_{fuel} = 1.5, λ_{air} = 2.2, 90/90% r.h. fuel/air input gas streams).

not change the cell performance dramatically in an all-parallel gas flow configuration with the given set of operating conditions.

4.1.2. All-serial gas flow configurations 5 and 6

The two all-serial stack setups 5 and 6, on the other hand, show significant variations in single cell output voltages and one common trend determining the individual cell performance within the stack, as shown in Fig. 6(c). The common trend among both stack setups is that the individual cell voltages are primarily determined by the hydrogen flow rate in the fuel gas stream. Cells located near the fuel inlet generally have high cell output voltages in co- as well as in counter-flow mode. Cell number four (i.e. the cell with the fuel inlet in both stack setups) therefore has the highest cell voltages in setups 5 and 6, respectively.

The gradual consumption of hydrogen along the anode flow direction, reducing the bulk flow velocity of the anode gas streams, leads to a significant reduction in cell output voltages. The fuel outlet cell number four has an output voltage <400 mV in both stack setups, whereas the fuel inlet cell number one has output voltages >600 mV at 25 A operation in both all-serial stack setups. A comparison of the two stack setups reveals a slight advantage of the co-flow stack setup 6 over the counter-flow stack setup 5, particularly with the fuel outlet cell number one. Cell operation is therefore clearly dominated by the hydrogen flow rate in the fuel gas stream; this can also be derived from the fact that the fuel inlet cells of stack setups 5 and 6 – being operated with very high values of hydrogen stoichiometry – have higher cell output voltages than in the all-parallel gas flow setups 1 and 2. The opposite effect is derived for the fuel outlet cells of the all-serial configurations. Here, the all-parallel gas flow stack setups performed better than the stacks with an all-serial flow configuration.

4.1.3. Mixed gas flow configurations 3 and 4

Cell voltages for the mixed gas flow setups 3 and 4 are compared in Fig. 6(b). As with the all-serial setups 5 and 6, the fuel inlet cells again have significantly higher cell output voltages than the fuel outlet cells. Stack setup 3 (four cells in parallel and one cell in serial gas flow configuration) has slightly higher averaged cells voltages than stack setup 4 (three cells in parallel and two cells in serial gas flow configuration). Due to the fact that the averaged cell output voltages measured with stack setups 3 and 4 are also higher than the averaged cell output voltages measured with the all-parallel setups 1 and 2, the mixed operation of cells in parallel and serial gas flow configuration seems beneficial – again for the investigated operating parameters and cell configurations – with respect to the averaged cell output voltage achieved with the investigated laboratory-scale PEMFC stack.

The reason for this could be that the fuel and air stoichiometry as well as the total gas pressure present with the inlet cells of stack setups 3 and 4 are (slightly) higher than with stack setups 1 and 2. This is due to the fact that the fuel and air gas streams for the cells operated in serial gas flow configuration (i.e. cell number five in stack setup 3 and cells number four and five in stack setup 4) have to be transported through the inlet cells operated in a parallel gas flow configuration (i.e. cells one to four in stack setup 3 and cells one to three in stack setup 4). The overall balance of water content in membrane and electrodes, the supply with fresh fuel and air as well as the slightly higher pressure drop obviously results in the average cell of the mixed serial/parallel stack setups 3 and 4 being operated more efficiently, i.e. with higher average cell output voltages—than in the all-parallel stack setups 1 and 2.

4.2. Individual cell and stack performance as a function of fuel and air input gas stream humidification

The water balance has a significant impact on performance, stability and lifetime of fuel cells. This is particularly true for low-temperature PEMFCs [27]. The protonic conductivity of polymer electrolyte membranes such as Nafion is proportional to the membrane water content [20]. Drying of the membrane during operation should therefore be avoided at all times in order to minimise the

membrane resistance and thus maximise the operational fuel cell output voltage.

Liquid water can either be produced within the cell (i.e. electrochemical product water generated within the cathode electrode active layer) or it can also be formed within the anode and cathode electrodes and flow fields (i.e. condensed water vapour). The presence of liquid water in electrodes and flow fields can result in significant gas transport limitations and thus cause a loss in operational fuel cell output voltage [28].

A good balance between dehydration of the polymer electrolyte membrane (membrane drying) and the formation of liquid water in the electrodes (electrode flooding) has therefore got to be found.

The water balance of PEMFCs is essentially governed by four key factors: water being transported into the cell or stack by the (externally) humidified input gas streams, product water generation by the electrochemical reaction proceeding within the cathode electrode active layer, cross-membrane liquid water transport from the anode to the cathode electrode due to electro-osmotic drag, and back-diffusion of liquid water from the cathode to the anode electrode due liquid water concentration gradients [20,29].

Ciureanu [29] found that for a stack being operated with external cathode input gas humidification, the membrane resistance is comparably small and not strongly linked to the presence of an external anode input gas stream humidification. If the stack is operated with a dry cathode input gas stream, however, the membrane resistance is high at low current densities and decreases only with an increase in current densities and thus a higher product water generation rate.

Ciureanu also found a significant increase in membrane resistance after intermittently cutting off the cathode input gas stream humidification, and a relatively small increase in membrane resistance after intermittently cutting off the anode input gas stream humidification. The resistance of the polymer electrolyte membrane is therefore primarily dominated by the water concentration at the cathode electrode/membrane interface. We therefore chose to apply external cathode input gas humidification with all three input gas humidification cases investigated within this study.

The current/voltage characteristics measured for the humidification-dependent investigations were made at a stack temperature of 70 °C, a hydrogen stoichiometry of 1.5 and an air stoichiometry of 2.2. Three different input gas humidification cases were investigated: 0/90%, 60/60%, 90/90% r.h. of the fuel/air input gas streams. Results of these investigations are compiled in Fig. 7(a–c) for all six stack setups and stack output currents of 0 A (OCV mode), 5 A and 20 A.

4.2.1. OCV mode operation

The OCV mode plot, Fig. 7(a), shows that the mixed parallel/serial stack setups 3 and 4 have the highest OCVs at all three investigated humidification cases. The all-serial stack setups 5 and 6 have slightly smaller OCVs and the all-parallel stack setups 1 and 2 have the lowest OCVs. The reason why the all-parallel stack setups have the lowest OCVs might be that a smaller pressure drop is required to push the fuel and air gas streams through an all-parallel stack setup than through a stack setup with a serial configuration. The fact that the stack setups featuring an all-serial gas flow configuration – having the largest pressure drop of all investigated stack setups (stack setups 5 and 6) – do not have the highest OCVs indicates that gas pressure levels alone cannot explain the differences in OCVs. A more complex interdependence between OCVs, fuel and air gas pressures and membrane water content therefore suggests itself.

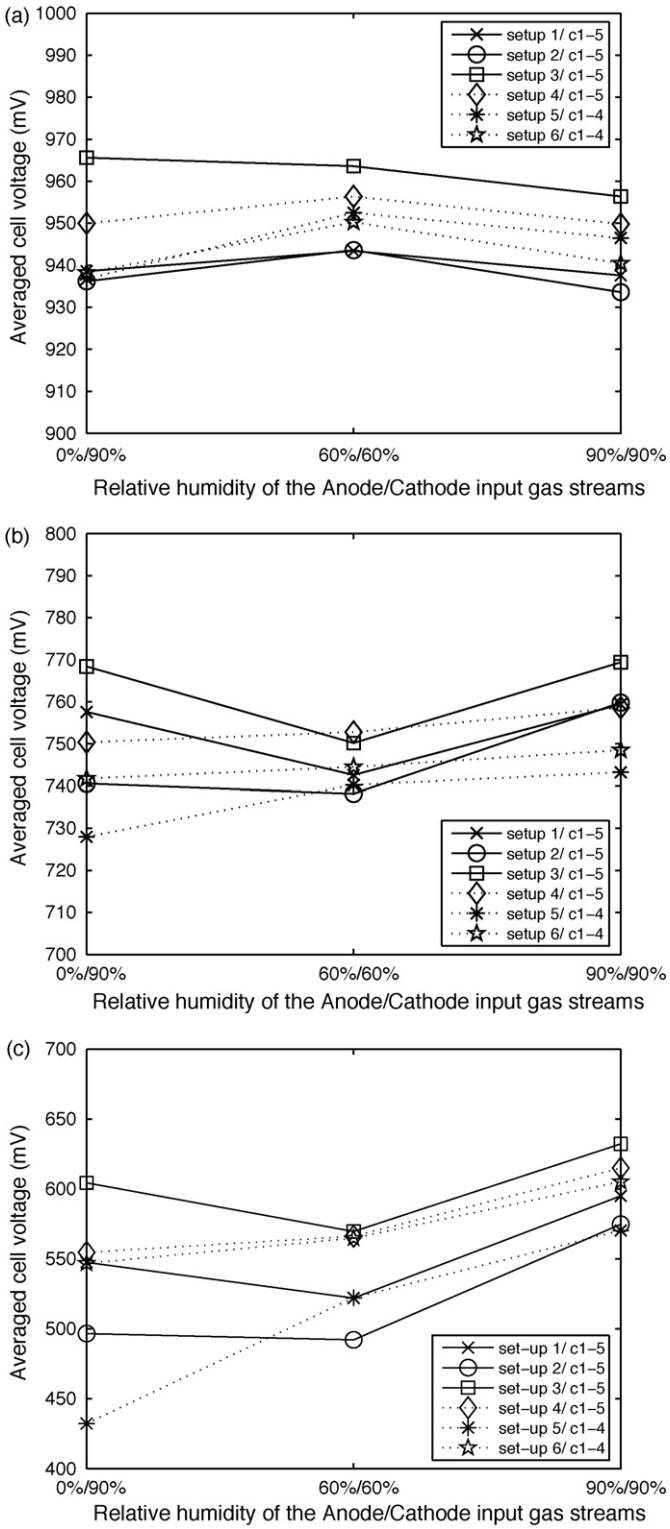

Fig. 7. Comparison of averaged cell output voltages for the six stack setups and 0 A (a), 5 A (b) and 20 A (c) output current (70 °C stack temperature, $\lambda_{fuel} = 1.5$, $\lambda_{air} = 2.2$).

4.2.2. Low current density operation

Two general trends can be derived from the measurements made for stack operation with a net stack output current: firstly, there are obviously two groups of stack setups. Group one consists of stack setups 3, 1 and 2 (written in the order of magnitude of the average cell output voltage). Group two consists of stack setups 4,

6 and 5 (again written in the order of the magnitude of the average cell output voltage).

The average cell output voltage of the group one setups at 5 A and 20 A output current show V-like characteristics in the humidity-dependent plots, as shown in Fig. 7(b) and (c). Peak output voltages of the group one stack setups are derived for the measurements made at 90/90% relative humidity of the fuel/air input gas stream, followed by the 0/90% measurements. The smallest cell output voltages are derived for the 60/60% measurements.

Stack setups 1–3 are primarily parallel gas flow-dominated stack setups (setups 1 and 2 are all-parallel gas flow configurations, setup 3 has four cells in parallel and only one cell in serial gas flow configuration). Due to the lack of a strong serial gas flow component, the water balance of the cells is therefore obviously governed by the external humidification of the air input gas stream. The average cell output voltage of the group one stack setups thus seems to be governed by air input gas humidification. Only a minor dependence on fuel input gas humidification is present. This can be seen in the 5 A plot (Fig. 7b) and even more so in the 20 A plot (Fig. 7c) where the average cell output voltages measured for 0/90% are slightly smaller than for 90/90% due to the aforementioned relevance of fuel input gas humidification with high output current operation of the fuel cell stack.

External humidification of the fuel input gas stream is therefore primarily required with the investigated parallel gas flow-dominated stack setups if high output currents are drawn from the cell. This goes in line with the current understanding of water transport models developed for low-temperature polymer electrolyte membranes such as Nafion, predicting a dehydration of the anode electrode/membrane interface at high current density operation due to electro-osmotic drag of water molecules from the anode to the cathode electrode [20–22].

Slightly different results are derived for the second group, the serial gas flow-dominated stack setups 4, 5 and 6 (5 and 6 are all-serial configurations, 4 has three cells in parallel and two cells in serial gas flow configuration). In case of this group of stack setups, minimum cell output voltages are derived for the 0/90% case, medium output voltages are derived for the 60/60% case and maximum output voltages are again derived for the 90/90% case.

Contrary to what is derived for the parallel gas flow-dominated stack setups, a lack of fuel input gas humidification directly results in a significant reduction of the average cell output voltage. This is an unexpected result, as one might have suspected that a reduced input gas humidification would be beneficial with serial gas flow-dominated setups due to the significant product water uptake along the gas flow through the cells particularly at high current density operation. This is obviously not the case with the measured characteristics of the serial gas flow-dominated stack setups, as the maximum input gas humidification rates of the fuel and air gas streams also result in the maximum cell output voltages with the serial gas flow-dominated stack setups.

4.2.3. High current density operation

At high current density operation, fuel input gas stream humidification seems to be particularly important for the serial gas flow-dominated stack setups 4–6. The parallel gas flow-dominated stack configurations 1–3 only show a slight dependence on anode input gas humidification with high current density operation, as mentioned above. This difference between serial and parallel gas flow-dominated stack setups is due to the complex interaction between input gas humidification and product water uptake as well as membrane water content and electrode flooding presented in Fig. 1.

This can also be seen when comparing the individual cell output voltages of stack setups 5 and 6 for 90/90% input gas humidification, shown in Fig. 6c, and 0/90% input gas humidification shown in Fig. 8. Stack configurations and operating conditions are identical, the only difference between these two plots is the presence (Fig. 6c) or lacking (Fig. 8) of external fuel input gas stream humidification.

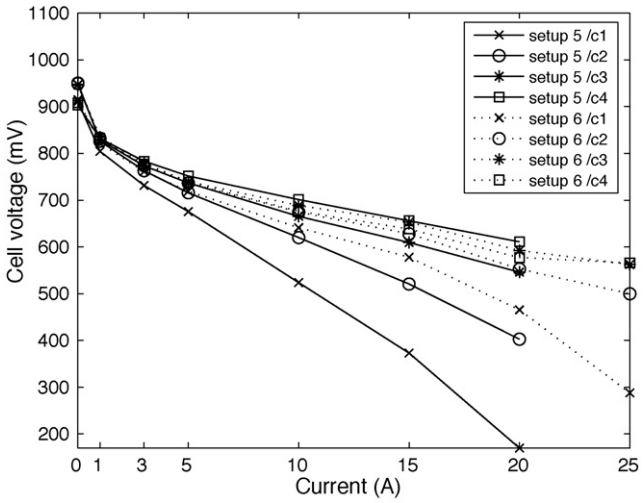

Fig. 8. Comparison of single cell output voltages for stack setups 5 and 6 (70 °C stack temperature, $\lambda_{fuel} = 1.5$, $\lambda_{air} = 2.2$, 0/90% r.h. fuel/air).

In Fig. 6c, the single cell voltages for stack setups 5 and 6 are compared for 90/90% relative humidity of the fuel/air input gas streams. The output voltages of the individual cells are primarily governed by the hydrogen content of the fuel gas stream, as discussed above. Cell number four (the fuel inlet cell) has the highest output voltages in both stack setups 5 and 6, whereas cell number one (the fuel outlet cell) has the lowest output voltages. Cell output voltages measured with stack setup 5 (counter-flow mode) are slightly smaller than those measured with stack setup 6 (co-flow mode).

Similar characteristics are also derived with the 0/90% relative humidity measurements of stack setups 5 and 6 shown in Fig. 8. In case of dry fuel input gas stream operation (i.e. without fuel input gas stream external humidification), the performance of the individual cells is generally lower than with external fuel input gas stream humidification (Fig. 6c). Stack setup 5 (counter-flow mode) is again slightly better than stack setup 6 (co-flow mode).

One major difference can be derived from the current/voltage characteristics plotted in Fig. 8: the cell voltage of fuel outlet cell number one of stack setup 5 (counter-flow mode) is almost 300 mV smaller than with stack setup 6 (co-flow mode) at an output current of 25 A. The fuel outlet cell of stack setup 5 receives the fresh input air stream and the fuel gas stream previously fed through cells one to three. The combination of a fresh air gas stream (no product water uptake from upstream cells) and the initially dry fuel input gas stream previously passing through cells one to three before being fed into cell four obviously results in the presence of significant membrane drying effects in cell number one, and – to a smaller degree – also in cell number two. These membrane drying effects result in a very large ohmic drop across the membrane, as can be seen in Fig. 8 where the linear region of cell number one of stack setup 5 is significantly sharper declined than with the same cell operated in stack setup 6.

The cell output voltage available with cells number one and two in stack setup 5 (counter-flow mode) at high output current operation is thus significantly smaller than with stack setup 6 (co-flow mode).

These strong interactions between water balance and gas streams can be directly seen in a serial gas flow configuration, where product water generation, water uptake by the air gas stream

and cross-membrane liquid water transport phenomena are locally separated by the utilisation of individual cells. In a parallel gas flow configuration, similar phenomena will not occur between individual cells, but between the inlet and outlet region of each cell. The magnitude of this effect is, however, often reduced due to the presence of a single membrane, and the possibility of choosing flow field patterns with the anode and cathode electrode that aid in distributing the membrane water content – as well as the current density distribution – over the active cell area as evenly as possible.

Applying a prudent flow field design for the anode and the cathode electrode, the operation of a PEMFC can be made more homogenously, e.g. by avoiding strong cross-membrane liquid water transport from the anode to the cathode electrode that might result in dehydration of the anode electrode/membrane interface. This can obviously not be made when a number of individual cells are arranged in a serial gas flow configuration.

This is one of the most important differences between a serial and a parallel gas flow-dominated fuel cell stack configuration: in a parallel gas flow-dominated stack configuration, fuel and air supply as well as water balance essentially have to be solved and optimised on cell-level. This is not the case with a serial gas flow-dominated stack configuration: fuel and air supply as well as each cell's water balance do not only have to be solved appropriately on cell but also on stack-level, as each individual cell operated in a serial gas flow configuration is directly affected by the operation of each upstream cell, and directly affects the operation of each downstream cell. This makes a prudent stack design more challenging, particularly if the stack is supposed to be operated dynamically with quickly changing electric load requirements.

4.3. Individual cell and stack performance as a function of air stoichiometry

The air stoichiometry generally has a significant impact on the water balance of low-temperature PEMFCs, particularly in removing electrochemical product water generated in the cathode electrode active layer out of the cell assembly. Low-temperature PEMFCs are therefore often operated with relatively high air stoichiometry rates in order to provide cell operation in a stable (e.g. no fluctuations in cell output voltage due to intermediate or permanent blocking of individual gas channels in the anode and cathode flow fields) and efficient (i.e. maximum output voltages) way [30].

The stoichiometry of the air gas stream has a direct impact on fuel cell performance not only by supplying fresh oxygen to the electrochemically active sites, but also by influencing the water content of the polymer electrolyte membrane and – primarily at high current density operation – causing or removing electrode flooding effects within the cathode electrode [1].

In order to analyse the effect of air stoichiometry on individual cell and stack operation, the averaged cell output voltages for all six investigated stack configurations are presented in Fig. 9(a) and (b) for output currents of 5 A and 20 A. The current/voltage characteristics were again made at a stack temperature of 70 °C and 90/90% relative humidity of the fuel/air input gas streams. A constant hydrogen stoichiometry of 1.5 was applied with all measurements; the oxygen stoichiometry was set to values of 1.4, 1.8, 2.2, 2.6 and 3.0.

4.3.1. Low current density operation

An increase in averaged cell output voltages with air stoichiometry is derived with most investigated stack setups. A slight difference is derived between all-parallel and mixed gas flow configurations (i.e. stack setups 1–4) and all-serial gas flow configurations (i.e. stack setups 5 and 6). All-serial gas flow configurations tend to show a significant and gradual increase in averaged cell voltages with air stoichiometry at low current density operation, as shown in the 5 A plot presented in Fig. 9(a).

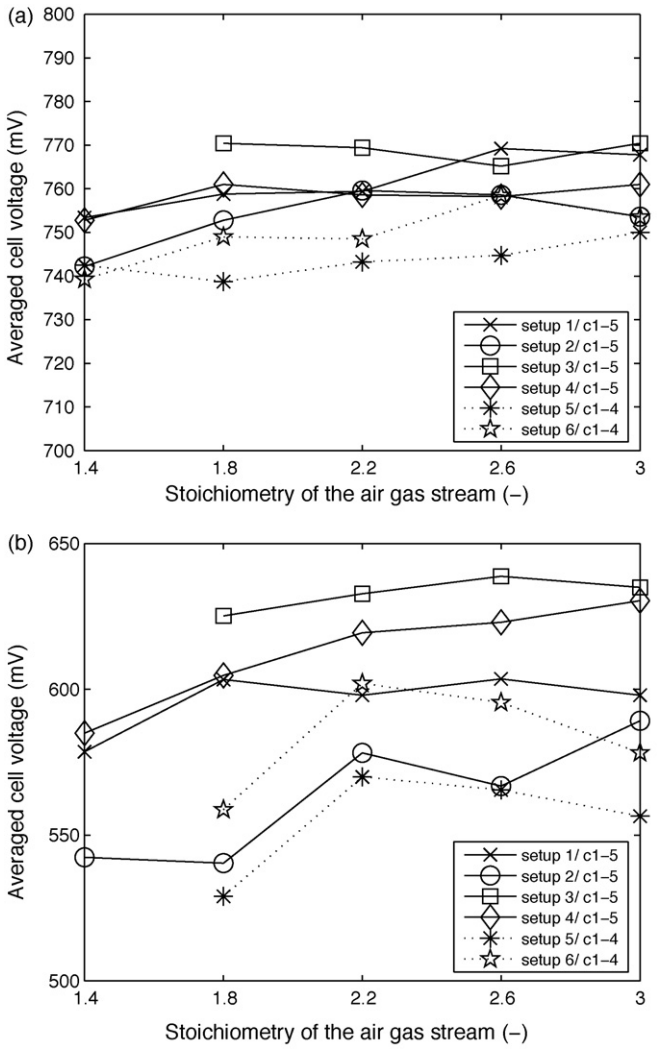

Fig. 9. Comparison of single cell output voltages for stack setups 1–6 and stack currents of 5 A (a) and 20 A (b) (70 °C stack temperature, λ_{fuel} = 1.5, 90/90% r.h. fuel/air).

The average cell output voltages of the all-parallel and mixed gas flow configurations also increases with air stoichiometry in case of 5 A output current operation, but this increase is less significant than with the all-serial gas flow configurations. Cell output voltages even tend to peak at rather low stoichiometry rates with the all-parallel and mixed gas flow stack setups, and become slightly smaller when even higher stoichiometry rates are applied. Choosing high values of air stoichiometry does therefore not necessarily lead to an increase in cell output voltages in case of the all-parallel and mixed gas flow configurations. This is even more so when considering that an increase in air stoichiometry will also result in a higher auxiliary load of the air compressor.

The variation of stack performance with air stoichiometry seems to be governed by the interdependence between oxygen supply and water balance of the individual cells. In an all-serial gas flow configuration, the air stream has to remove the product water from all of the cells that are connected in series (most of the product water is normally removed by the air stream due to the fact that the product water is generated within the cathode electrode, and the air stoichiometry is normally significantly higher than the fuel stoichiometry). An increase in air stoichiometry will therefore tend

to remove more product water out of the cells, and the cell performance will thus normally tend to benefit from the improved supply with fresh oxygen.

An increase in air stoichiometry will therefore rather improve the overall stack performance in a serial gas flow-dominated stack setup. This assumption is supported by the averaged cell output voltage curves of the all-serial gas flow setups 5 and 6 shown in Fig. 9a that increase gradually with the air stoichiometry. The absolute increase in averaged cell output voltages of approximately 10–15 mV for an increase in air stoichiometry from 1.4 to 3 derived with stack setups 5 and 6 is rather small in case of the 5 A measurement, though.

In case of the parallel gas flow-dominated stack configurations and 5 A operation, an increase in air stoichiometry does not necessarily lead to an increase in cell performance as product water removal is not such a major challenge as with an all-serial gas flow configuration. In a parallel gas flow-dominated configuration, the benefit of an improved supply with fresh oxygen is rather counterbalanced by the negative effects of a higher rate of electrochemical product water removal. The average membrane water content could thus be effectively reduced by an increase in air stoichiometry. This would explain why the average cell output voltages of some parallel gas flow-dominated fuel cell stack configurations peak at medium values of air stoichiometry, and the average cell output voltages rather tend to be reduced with a further increase in air stoichiometry.

This assumption is supported by the fact that this difference between serial and parallel gas flow-dominated stack configurations is particularly relevant with small and medium current densities where the product water generation rate is rather small and electrode flooding is therefore not a major issue, particularly not with an all-parallel gas flow configuration.

4.3.2. High current density operation

At high current density operation, the performance of the parallel and mixed gas flow configurations gradually improves with an increase in air stoichiometry. This can be seen particularly well with the output voltage curves of stack setups 2–4 plotted in Fig. 9b. The output voltage of stack setup 1 does not show this gradual increase in output voltage, as the output voltage rather peaks at an air stoichiometry of 1.8 and remains almost constant at higher air stoichiometry rates.

The improved product water removal associated with an increase in air stoichiometry therefore seems to be beneficial with all-parallel and mixed gas flow configurations at high current density operation, and an increase in air stoichiometry from 1.4 to 3.0 leads to an increase in averaged cell output voltages in the order of 50 mV with stack setups 2 and 3, for instance.

4.3.3. Comparison of the current/voltage characteristics of an all-parallel gas flow configuration for medium and high air stoichiometry operation

The averaged cell current/voltage characteristics of stack setup 1 (all-parallel, counter-flow mode) is compared for an air stoichiometry of 2.2 and 3 in Fig. 10. The higher air stoichiometry results in a slight drop in cell output voltages in low current density operation. This goes in line with the above discussion of the 5 A case presented in Fig. 9a. The output voltages are roughly identical for output currents between 15 A and 20 A. Cell output voltages at high current density operation are improved by applying the higher air stoichiometry rate, as discussed with the high output current plot shown in Fig. 9b.

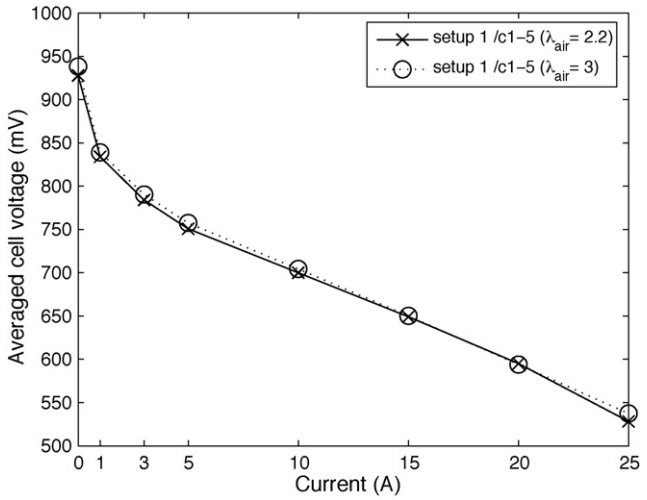

Fig. 10. Comparison of single cell output voltages for stack setup 1 (70 °C stack temperature, λ_{fuel} = 1.5, 90/90% r.h. fuel/air).

4.3.4. Comparison of the current/voltage characteristics of an all-serial gas flow configuration for medium and high air stoichiometry operation

The opposite effect is derived for all-serial gas flow configurations. Here, the general trend of a gradual increase in averaged cell output voltages with air stoichiometry derived with small current densities is reversed with high current density operation. At high current density operation, an increase in air stoichiometry results in a slight reduction of the averaged cell output voltages, as can be seen with the current/voltage characteristics of stack setup 5 for operation with air stoichiometry rates of 2.2 and 3. Peak output voltages are achieved at an air stoichiometry rate of 2.2, and a further increase in air stoichiometry results in a slight reduction of the individual and stack-averaged cell output voltages. The reason for this effect might again be based on water balance and cross-membrane water transport characteristics. The difference between operating stack setup 5 with air stoichiometry rates of 2.2 and 3.0 is, however, again rather small, as shown in Fig. 11.

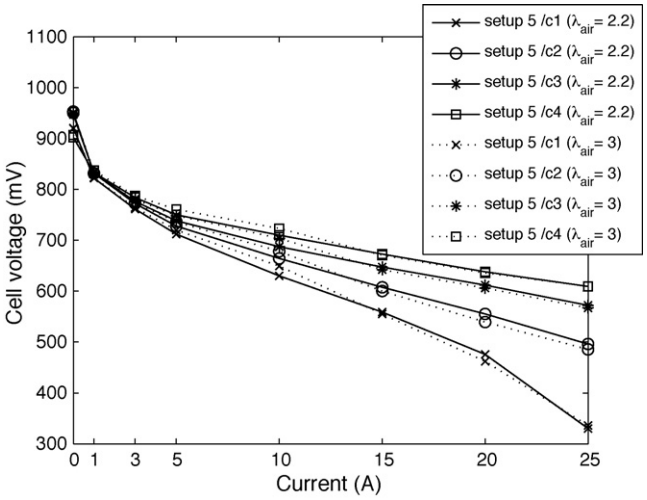

Fig. 11. Comparison of single cell output voltages for stack setup 5 (70 °C stack temperature, λ_{fuel} = 1.5, 90/90% r.h. fuel/air).

5. Conclusions

The interdependence between air stoichiometry rates, fuel and air input gas stream humidification levels and internal gas flow configurations of a laboratory-scale PEMFC stack are investigated within this paper. The investigations revealed that the internal gas flow configuration has a significant impact on operation and performance of the individual cells installed within the stack, as well as on the operational characteristics of the fuel cell stack, respectively.

Of the six stack setups investigated, the two mixed gas flow setups 3 and 4 (parallel gas flow configuration of four/three cells with one/two cells in a serial gas flow configuration) showed the highest average cell output voltages in the majority of measurements. The two all-parallel gas flow stack setups 1 and 2 (parallel gas flow configuration of five cells in counter-/co-flow mode) showed slightly smaller average cell output voltages, whereas the all-serial stack setups 5 and 6 (serial gas flow configuration of four cells in counter-/co-flow mode) had the lowest average output voltages. This ranking of internal stack gas flow configurations is valid over a wide range of operating conditions (i.e. stoichiometry rates of the air input gas stream, relative humidity of the fuel and air input gas streams).

A detailed analysis of the fuel cell stack performance as a function of operating conditions was subsequently made in order to analyse and compare operational characteristics of the six investigated internal gas flow configurations in detail. Measurements made with three different input gas humidification levels and five different air stoichiometry rates revealed the complex interdependence between reactant supply, membrane drying and electrode flooding that governs operation and performance of the individual cells and the fuel cell stack assembly, respectively.

The performance of each cell operated within a fuel cell stack is strongly influenced by the supply with fresh reactants as well as the water balance between electrochemical product water generation, input gas humidification and product water removal. Analysis and optimisation of operational performance can only be simultaneously made on individual cell- and stack-level with an all-parallel gas flow configuration, though. With an all-serial or mixed serial/parallel gas flow configuration, fuel and air supply as well as water balance do not only have to be provided appropriately on cell- but also on stack-level, as each individual cell operated in a serial gas flow configuration is directly affected by the operation of each upstream cell, and directly affects the operation of each downstream cell. This makes a prudent stack design more challenging, particularly if the stack is supposed to be operated dynamically and can therefore not be optimised for stationary operation with pre-defined operating conditions.

Acknowledgements

The authors appreciate the support of the Austrian Federal Ministry for Transport, Innovation and Technology (BMVIT) and the Austrian Research Promotion Agency (FFG).

References

[1] Q. Yan, H. Toghiani, H. Causey, J. Power Sources 161 (2006) 492–502.
[2] J. Park, X. Li, J. Power Sources 162 (2006) 444–459.
[3] P.A.C. Chang, J. St. Pierre, J. Stumper, B. Wetton, J. Power Sources 162 (2006) 340–355.
[4] J.-H. Koh, H.-K. Seo, C.G. Lee, Y.-S. Yoo, H.C. Lim, J. Power Sources 115 (2003) 54–65.
[5] J.P. Owejan, T.A. Trabold, J.J. Gagliardo, D.L. Jacobson, R.N. Carter, D.S. Hussey, M. Arif, J. Power Sources 171 (2007) 626–633.
[6] S.Y. Kim, W.N. Kim, J. Power Sources 166 (2007) 430–434.
[7] C.-Y. Chena, W.-H. Lai, B.-J. Weng, H.-J. Chuang, C.-Y. Hsieh, C.-C. Kung, J. Power Sources 179 (2008) 147–154.
[8] X. Zhang, D. Zheng, T. Wang, C. Chena, J. Caoa, J. Yan, W. Wang, J. Liu, H. Liu, J. Tian, X. Li, H. Yang, B. Xia, J. Power Sources 166 (2007) 441–444.
[9] Z. Qi, H. Tang, Q. Guo, I. Du, J. Power Sources 128 (2004) 208–217.
[10] W.R. Baumgartner, O. Parz, S.D. Fraser, E. Wallnöfer, V. Hacker, J. Power Sources 182 (2008) 413–421.
[11] B. Wahdame, D. Candusso, X. François, F. Harel, M.-C. Péra, D. Hissel, J.-M. Kaufmann, Int. J. Hydrogen Energy 32 (2007) 4523–4536.
[12] A.C. Fisher, Electrode Dynamics, Oxford University Press, Oxford, 1996, pp. 1–3.
[13] C.H. Hamann, W. Vielstich, Elektrochemie, third ed., Wiley–VCH, Weinheim, 1998, pp. 175–193.
[14] D. Pletcher, A First Course in Electrode Processes, The Electrochemical Consultancy, Romsey, 1991, pp. 28–32.
[15] H. Dohle, A.A. Kornyshev, A.A. Kulikovsky, J. Mergel, D. Stolten, Electrochem. Commun. 3 (2001) 73–80.
[16] A.A. Kulikovsky, Electrochem. Commun. 4 (2002) 527–534.
[17] J. Larminie, A. Dicks (Eds.), Fuel Cell Systems Explained, second ed., Wiley, Chichester, Weinhein, New York, Brisbane, Singapore, Toronto, 2003, pp. 69–81.
[18] J.J. Baschuk, X. Li, J. Power Sources 86 (2000) 181–196.
[19] P. Berg, K. Promislow, J. St. Pierre, J. Stumper, B. Wetton, J. Electrochem. Soc. 151 (2004) A341–A353.
[20] T.E. Springer, T.A. Zawodzinski, S. Gottesfeld, J. Electrochem. Soc. 138 (1991) 2334–2342.
[21] D.M. Bernardi, M.W. Verbrugge, J. Electrochem. Soc. 139 (1992) 2477–2490.
[22] S.D. Fraser, M. Monsberger, V. Hacker, ECS Trans. 1 (2006) 399–408.
[23] T. Mennola, M. Mikkola, M. Noponen, T. Hottinen, P. Lund, J. Power Sources 112 (2002) 261–272.
[24] W.R. Baumgartner, E. Wallnöfer, T. Schaffer, J.O. Besenhard, V. Hacker, V. Peinecke, P. Prenninger, Electrochem. Soc. Trans. 3 (2006) 811–825.
[25] W.R. Baumgartner, Characterisation of PEM Fuel Cells, Dissertation, Graz University of Technology, 2007.
[26] B. Hebenstreit, Development and Characterization of a Polymer-Electrolyte-Membrane Fuel Cell Stack, Diploma Thesis, Graz University of Technology, 2007.
[27] J.-M. Le Canut, R.M. Abouatallah, D.A. Harrington, J. Electrochem. Soc. 153 (2006) A857–A864.
[28] A. Hakenjos, M. Zobel, J. Clausnitzer, C. Hebling, J. Power Sources 154 (2006) 360–363.
[29] M. Ciureanu, J. Appl. Electrochem. 34 (2004) 705–714.
[30] B. Wahdame, D. Candusso, J.-M. Kauffmann, J. Power Sources 156 (2006) 92–99.